Received: 1 December 2021 | Revised: 31 March 2022 | Accepted: 25 April 2022

DOI: 10.1002/pen.26018

RESEARCH ARTICLE

POLYMER ENGINEERING AND SCIENCE WILEY

Composition-dependent glass transition temperature in mixtures: Evaluation of configurational entropy models

Evelyn Lopez[1] | **Yung P. Koh**[2] | **John A. Zapata-Hincapie**[1] | **Sindee L. Simon**[2]

[1]Department of Chemical Engineering, Texas Tech University, Lubbock, Texas, USA

[2]Department of Chemical and Biomolecular Engineering, North Carolina State University, Raleigh, North Carolina, USA

Correspondence
Sindee L. Simon, Department of Chemical and Biomolecular Engineering, North Carolina State University, Raleigh, NC 27695, USA.
Email: slsimon@ncsu.edu

Funding information
National Science Foundation, Grant/Award Numbers: CMMI 1662046, DMR 1006972, DMR 2105065

Abstract

The composition dependence of the glass transition temperature (T_g) in mixtures remains an important unsolved problem. Here, it is revisited using three model systems: a series of oligomeric and polymeric cyanurates, blends of oligomeric and polymeric α-methyl styrene, and molecular mixtures of itraconazole and posaconazole. We evaluate several entropy-based models to determine the theoretical T_g as a function of molecular composition and compare the results against the experimental data. The assumption that the configurational entropy is invariant at the T_g is tested, where the change in configurational entropy is assumed to be given by the integral of $\Delta C_p d\ln T$, where ΔC_p is the temperature-dependent change in the heat capacity at T_g. We find that, although the temperature-dependent heat capacities in both liquid and glassy states are nearly independent of composition for several of the systems studied (i.e., they are nearly ideal mixtures), the composition dependence of T_g is not well described by simply adding the changes in the mass-weighted configurational entropy of the components on going from the T_g in the pure state to that of the blend. The implication is that either configurational entropy is not invariant at T_g or that it cannot be obtained from the integral of $\Delta C_p d\ln T$.

KEYWORDS

configurational entropy, glass transition temperature, mixtures, thermodynamics

1 | INTRODUCTION

The glass transition temperature (T_g) of miscible mixtures has been well investigated over the past 70 years,[1–13] and a number of relationships have been proposed, including those by Fox,[5] Gordon–Taylor,[6] Kelley–Beuche,[7] Couchman,[8–10] Venditti–Gillham,[11] Jenckel–Heusche,[12] Braun–Kovacs,[13] and Kwei.[14] The model equations, along with underlying assumptions, are shown in Table 1. The basis for these equations is that the configurational entropy S_c (or the free volume, depending on the derivation) is invariant at the glass transition, such that the governing equation for conservation of configurational entropy in the case of an ideal mixture in the thermodynamic sense (i.e., one in which there is no excess volume V^E or excess entropy S^E on mixing) is given by[8–10]

TABLE 1 Equations for the composition dependence of T_g[a]

Equation name(s)	Equation	Assumptions	Reference
Fox	$1/T_g = w_1/T_{g1} + w_2/T_{g2}$	$S_c(T_g) =$ constant $S^E = 0$ $T_{gi}\,\Delta C_{pi} =$ constant $\Delta C_{p1} = \Delta C_{p2}$	[5]
Gordon–Taylor; Kelley–Bueche	$T_g = \frac{x_1 T_{g1} + x_2 k T_{g2}}{x_1 + x_2 k}$	$S_c(T_g) =$ constant $S^E = 0$ $T_{gi}\,\Delta C_{pi} =$ constant	[6,7]
Couchman; Venditti–Gillham	$\ln T_g = \frac{x_1 \ln T_{g1} + x_2 k \ln T_{g2}}{x_1 + x_2 k}$	$S_c(T_g) =$ constant $S^E = 0$ $\Delta C_{pi} =$ constant	[8–11]
Braun–Kovacs; Jenckel–Heusch; Kwei	$T_g = \frac{x_1 T_{g1} + x_2 k T_{g2}}{x_1 + x_2 k} + q x_1 x_2$	$S_c(T_g) =$ constant $S^E \neq 0$ $T_{gi}\,\Delta C_{pi} =$ constant	[12–14]

[a]ΔSubscripts 1 and 2 refer to the species 1 and 2, w_i and x_i refer to the weight or mole fraction of component i, $k = \Delta C_{p2}/\Delta C_{p1}$, q is a constant, $S_c(T_g)$ is the configurational entropy at T_g, S^E is the excess entropy upon mixing, and ΔC_{pi} is the change in heat capacity at T_g for species i with units of J g^{-1} K^{-1} or J mol^{-1} K^{-1} depending on whether w_i or x_i are used in the equation.

$$\sum x_i \int_{T_{gi}}^{T_g} \Delta C_{pi} \mathrm{d}\ln T = 0 \tag{1}$$

where x_i is the fraction of component i in either mass or mole fraction depending on the units of the step change in heat capacity at T_g (ΔC_p), T_{gi} is the glass transition temperature of the component i, and T_g is the glass transition temperature of the mixture. The step change in heat capacity at T_g is given by the difference in the liquid and glass heat capacities: $\Delta C_p = C_{pl} - C_{pg}$, where C_{pl} is the temperature-dependent liquid heat capacity and C_{pg} is the temperature-dependent glass heat capacity. It is assumed that the total step change ΔC_p at T_g is due to losses in configurational degrees of freedom (rather than due to loss of vibrational or other degrees of freedom), or that the fraction of ΔC_p that is due to a loss of configurational degrees of freedom is independent of composition. Another implicit assumption in the original derivation by Gordon and coworkers[7] was that the configurational entropy went to zero at the ideal glass transition T_2 of Gibbs and DiMarzio,[15] which may not be the case according to a recent work by Xu et al.[16] Furthermore, Gordon and coworkers assumed that T_g and T_2 had the same composition dependence, which has been reported by Angell for aqueous electrolyte solutions,[17] but it is not the case for our work here as we show later. The restrictive assumptions made by Gordon et al. were not made in the later works of Couchman,[8–10] where the entropy of the mixture is simply assumed to be continuous at T_g. Although the equations shown in Table 1 were not necessarily first derived from configurational entropy ideas, the equations can be obtained from Equation (1) with appropriate assumptions, as summarized in Table 1. The Fox equation is obtained by assuming that $T_{gi}\Delta C_{pi}$ is a constant, with ΔC_{pi} having units of J g^{-1} K^{-1} and w_i being the weight fraction of component i. The Gordon–Taylor[6] or Kelly–Beuche[7] equations are obtained using the same assumption for the temperature dependence of ΔC_p, but now allowing for the two values to differ with their ratio expressed by the constant $k = \Delta C_{p2}(T_{g2})/\Delta C_{p1}(T_{g1})$. The Couchman[8–10] and Venditti–Gillham[11] equations further assume that ΔC_{pi} is independent of temperature, which is not typically the case, with the parameter k having the same meaning as in the Gordon–Taylor equation. Finally, the Jenckel–Heusch[12] and Kwei[14] equations, and the closely related Braun–Kovacs[13] equation, can be obtained by considering the Gordon–Taylor equation and adding a term qx_1x_2 that accounts for molecular interactions that give rise to excess entropy, enthalpy, and/or free volume. The generalization of Equation (1) for a nonideal mixture is

$$\sum x_i \int_{T_{gi}}^{T_g} \Delta C_{pi} \mathrm{d}\ln T + S_c^E = 0 \tag{2}$$

where the excess configuration entropy S_c^E can be assumed to have a form analogous to the one-parameter Margules model for the excess Gibbs free energy,[18] $S^E = Ax_1x_2$, where A is a constant. It is noted that this form is the same as the correction used in the Kwei model (qx_1x_2). Other more complicated expressions have also been used, especially for systems with stronger

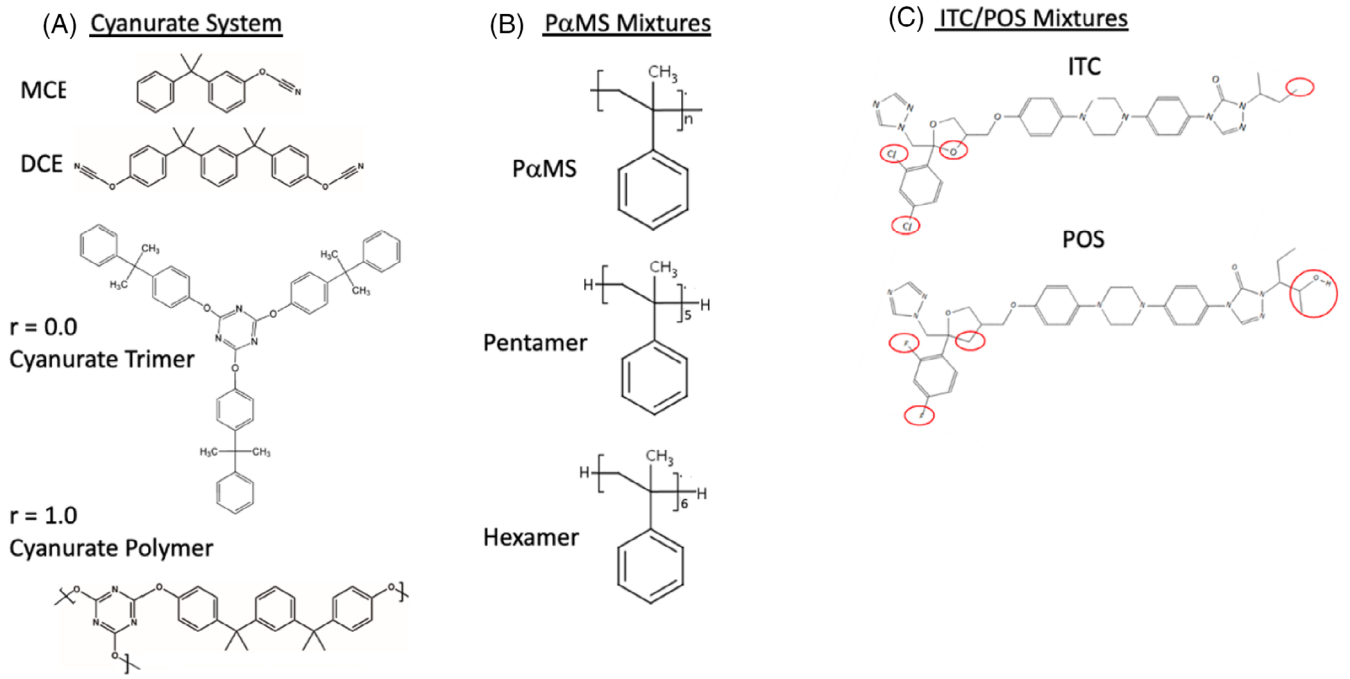

FIGURE 1 Chemical structure of (A) monocyanate ester (MCE) and dicyanate ester (DCE) used to synthesize cyanurate, the structure of which is also shown for $r = 0.0$ (trimer) and $r = 1.0$ (crosslinked polycyanurate); (B) poly(α-methyl styrene) (PαMS) and its pentamer or hexamer oligomer; and (C) itraconazole (ITC) and posaconazole (POS), with differences indicated in red circles.

intermolecular interactions in which excess enthalpic effects are considered,[19,20] systems where phase separation occurs,[21] and systems where the T_gs of the two components are very different[22]; however, these models are not of interest here because our aim is to examine nearly ideal miscible systems in which intermolecular interactions do not vary appreciably with composition.

Here, we examine the relationship between T_g and composition in three homologous near-ideal systems. For two of the systems, oligomeric/polymeric cyanurates and poly-(α-methyl styrene)/oligomer mixtures, absolute heat capacity data are used to directly test Equation (1) (for the first time, to the best of our knowledge). A third system, that of molecular mixtures of itraconazole (ITC) and posaconazole (POS) is also examined in order to extend the analysis to near-ideal mixtures of molecular glass-formers. In addition to T_g, the dynamic fragility, which can be measured using the cooling rate dependence of T_g,[23–26] is also reported here for the various systems. Fragility is often inversely correlated with the propensity of the material to pack efficiently during cooling; for example, small-molecule glass formers that pack efficiently are usually strong, whereas polymers are highly fragile.[27–33] Additionally, fragility usually increases with glass transition temperature for small molecules and polymeric glass formers[31]; however, there are known exceptions to that trend for polymers[30,34] and chalcogenides with varying degree of network rigidity.[35,36]

2 | EXPERIMENTAL METHODOLOGY

2.1 | Materials

Three homologous systems of varying composition are used for this investigation. The first is a series of cyanurates obtained by fully reacting mixtures of monofunctional cyanate ester (MCE) 4-cumylphenol cyanate ester (Oakwood Products) and difunctional cyanate ester (DCE), bisphenol M dicyanate ester (Hi-Tek Polymers). The molecular structures of MCE and DCE monomers are shown in Figure 1A. Eight formulations were made, each characterized by r, the mole fraction of cyanate ester groups that belong to the difunctional DCE monomer:

$$r = \frac{2N_D}{2N_D + N_M} \tag{3}$$

where N_D and N_M are the number of moles of the DCE and MCE monomers in the mixture, respectively. The formulations range from pure MCE ($r = 0.0$), which forms a cyanurate trimer having a molecular weight of 711 g/mol, to pure DCE ($r = 1.0$) which forms a crosslinked polycyanurate, and include six other formulations for which r ranges from 0.30 to 0.95. Each of the formulations studied was isothermally reacted to completion at 180°C under a nitrogen atmosphere, consistent

TABLE 2 Molecular weights, T_g, and ΔC_p for cyanurate series

	GPC data		Theoretical calculation			DSC data[a]	
r	M_w (g/mol)	M_n (g/mol)	M_w (g/mol)	M_n (g/mol)	X_c (mol/mol OCN)	T_g (°C)	ΔC_p ($Jg^{-1}K^{-1}$)
0.00	933	881	711	711	0	42.9 ± 0.4	0.40 ± 0.01
0.30	1613	1128	1843	1102	0	56.7 ± 0.5	0.34 ± 0.01
0.50	5998	2005	6913	1838	0	89.1 ± 0.4	0.29 ± 0.01
0.60	14,468	2452	∞	∞	0.02	99.9 ± 0.2	0.28 ± 0.02
0.80	n/a	n/a	∞	∞	0.18	121.0 ± 1.1	0.25 ± 0.02
0.85	n/a	n/a	∞	∞	0.22	146.0 ± 0.4	0.25 ± 0.01
0.95	n/a	n/a	∞	∞	0.30	171.0 ± 0.3	0.23 ± 0.01
1.00	n/a	n/a	∞	∞	0.33	190.0 ± 0.4	0.22 ± 0.02

[a]At 10 K/min heating after cooling at the same rate.

with the known reaction kinetics of MCE and DCE.[37,38] Completion of the reactions was confirmed by Fourier transform infrared spectrometer (FTIR), as shown in the SI. NMR was used to corroborate the r values (as shown in the SI), and gel permeation chromatography (GPC) was used to obtain the molecular weight of uncrosslinked formulations, as shown in Table 2, along with the expectations based on calculations using the Miller–Macosko recursive method,[39] which has been previously applied to polycyanurate systems.[37,40–43] Formulations for $r \geq 0.80$ were crosslinked and insoluble, and GPC data were not obtained. The theoretical calculation yields slightly lower molecular weights relative to the experimental values because of intracyclization in finite species.[41]

The second system of materials investigated consisted of blends of poly(α-methyl styrene) (PαMS) and its oligomer, either pentamer or hexamer, all obtained from Polymer Source Inc. (Dorval, Canada) and having narrow molecular weight distributions, as reported in a previous publication.[44] The oligomers purchased were synthesized such that the chain ends have the same chemical structure as the repeat unit in order to obtain ideal or near-ideal mixtures. Structures are shown in Figure 1B. The pure components were investigated, as well as mixtures with pentamer concentrations ranging from 2 to 98 wt% and mixtures with hexamer concentrations from 20 to 80 wt%. The absolute heat capacity for the pentamer mixtures was obtained by Huang, Simon, and McKenna and published in previous work,[44] those data were used by Simon and McKenna to conclude that an ideal glass transition as hypothesized by Gibbs and DiMarzio, does not exist.[45] The T_g and viscoelastic data for the hexamer mixtures were reported[46,47] and analyzed in the context of the Lodge–McLeish[48] self-concentration model. Here, we analyze the T_g data for the pentamer mixtures and extend the analysis to include the equations in Table 1 and numerical integration of Equation (1).

The third system investigated was that of itraconazole (ITC) and posaconazole (POS) mixtures, whose structures are shown in Figure 1C. Both ITC and POS with a purity higher than 99% were purchased from Sigma-Aldrich. ITC has smectic and nematic liquid crystal transitions,[49–51] as shown later, and thus, forms a smectic glass, whereas POS is amorphous with no liquid crystalline transitions. Mixtures with mass weight fractions from 0 to 100% ITC were sealed under nitrogen in 20 μl hermetic pans (PerkinElmer) having a pinhole in the lid. Samples were then dried in an oven at 140°C for 12 h prior to performing the experiments and stored in a desiccator when not in used.

3 | DSC MEASUREMENTS

A Perkin-Elmer Pyris 1 DSC with a freon intracooler system was used in step-scan mode to obtain the absolute heat capacities of the cyanurates and the PαMS blends. The step-scan method consists of multiple isothermal steps for 0.8 min each at intervals of 2 K with a heating ramp of 10 K/min used to go from one step to the next. In addition to the step-scan experiments, conventional heating scan experiments were also performed using the Perkin Elmer Pyris 1 DSC for the trimer cyanurate and using a Perkin-Elmer DSC7 with ethylene glycol cooling system for the higher molecular weight samples. A Mettler Toledo DSC 823e with a Julabo FT100 intracooler was used for the ITC/POS samples. All measurements were performed under a nitrogen atmosphere. DSC temperature calibration was accomplished using two calibration standards: indium and a liquid crystal (+)-4-n-hexylophenyl-40-(20-methylbutyl)-biphenyl-4-carboxylate (CE-3) for work on the cyanurates and ITC/POS materials, whereas indium and mercury were used as calibrants for the PαMS work. DSC heat flow was

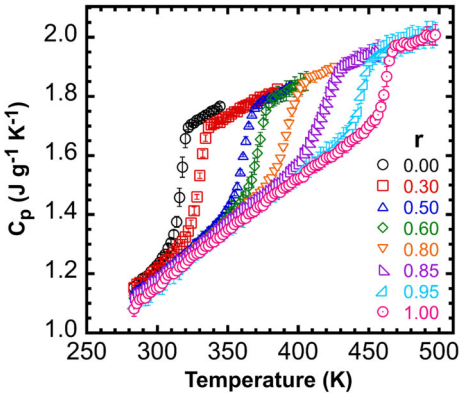

FIGURE 2 Absolute heat capacity curves of the fully reacted cyanurate series as a function of the fraction *r* of cyanate ester groups belonging to the difunctional cyanate. The data are the average of three runs of each sample with error bars indicating the standard deviation.

calibrated by indium, and absolute heat capacity was calibrated with sapphire with the measured heat capacity of the sapphire being reproduced to within 0.15%.

Heating scan experiments were performed to obtain the limiting fictive temperature (T_f') as a function of cooling rate using Moynihan's method[52]:

$$\int_{T_f'}^{T\gg T_f'} (C_{pl} - C_{pg})\mathrm{dT} = \int_{T\ll T_f'}^{T\gg T_f'} (C_p - C_{pg})\mathrm{dT} \qquad (4)$$

where C_p, C_{pl}, and C_{pg} are the heat capacity, liquid heat capacity, and glass heat capacity, respectively. The limiting fictive temperature is equivalent, within 1 K, to the glass transition temperature, which is obtained on cooling.[53] Consequently, T_g is used interchangeably with T_f' in the remainder of the text. The heating rate was kept constant at $\beta = 10$ K/min, while the cooling rates generally ranged from $q = 0.1$ to 30 K/min.

In addition to heating scan experiments performed using conventional DSC, a Mettler Toledo Flash DSC equipped with a freon intracooler and nitrogen purge was used to analyze the T_g over a larger cooling rate range for the cyanurate materials and for the itraconazole. The heating rate was kept constant at $\beta = 600$ K/s and the cooling rates ranged from $q = 0.1$ to 1000 K/s. Since the limiting fictive temperature does not depend on heating rate but only on cooling rate, the Flash data can be combined with the conventional DSC data. The Flash DSC was calibrated using the T_g values obtained from the conventional DSC T_g after cooling at 10 K/min for the cyanurates and using the value of the nematic liquid crystal transition for the ITC sample, as well as correcting for the thermal gradient in the latter sample using the methodology of Schawe.[54]

4 | RESULTS

The absolute heat capacities of the series of fully reacted cyanurates are shown in Figure 2. The glass transition temperature, T_g, increases and the heat capacity step change at T_g (ΔC_p) decreases with increasing dicyanate ester content (r). This trend is expected since molecular weight increases with increasing dicyanate ester content, and after gelation, crosslink density X_c also increases, as shown in Table 2. Interestingly, the absolute heat capacity data indicate that all of the cynanurates have very similar heat capacities, and although they are strongly temperature dependent, to a good approximation, they are independent of composition, indicating near ideal interactions between the MCE and DCE monomers. The liquid heat capacity (C_{pl}) data can be fit by a single second-order polynomial for $r \geq 0.30$, as shown in Figure 3A:

$$C_{pl}\left(\mathrm{Jg^{-1}K^{-1}}\right) = 0.50397 + 4.6433 \times 10^{-3}T - 3.2399 \times 10^{-6}T^2 \qquad r \geq 0.3 \qquad (5)$$

where T has units of K. The average standard deviation between the data points and the fit is 0.0056 Jg^{-1} K^{-1} (0.3%) and the maximum standard deviation is 0.014 Jg^{-1} K^{-1} (0.7%). The liquid heat capacity of the trimer cyanurate ($r = 0.0$) is higher than C_{pl} of the other formulations by 0.04036 Jg^{-1} K^{-1}:

$$C_{pl}\left(\mathrm{Jg^{-1}K^{-1}}\right) = 0.54433 + 4.6433 \times 10^{-3}\mathrm{T} - 3.2399 \times 10^{-6}T^2 \quad r = 0.00 \qquad (6)$$

The glassy heat capacity (C_{pg}) is also a quadratic function of temperature which shifts upward with increasing monofunctional content, as shown in Figure 3B for C_{pg} determined at 300 K (26.8°C). The data as a function of composition (r) and temperature are well described by

$$C_{pg}\left(\mathrm{Jg^{-1}K^{-1}}\right) = -0.19277 - 0.061132\,r + 5.5165 \times 10^{-3}T - 2.6457 \times 10^{-6}\,T^2 \qquad (7)$$

where T has units of K. Interestingly, Satoh's group contribution method[55] also gives a reasonable description of the glassy data, as shown in Figure 3B.

The T_g versus composition relationship for the cyanurates as a function of dicyanate ester content (r) is shown in Figure 4. T_g in this system monotonically increases from a value of 42.9 ± 0.4°C for $r = 0.0$ to 189.7 ± 0.3°C for $r = 1.0$. The prediction from configurational entropy conservation (Equation 1) was determined

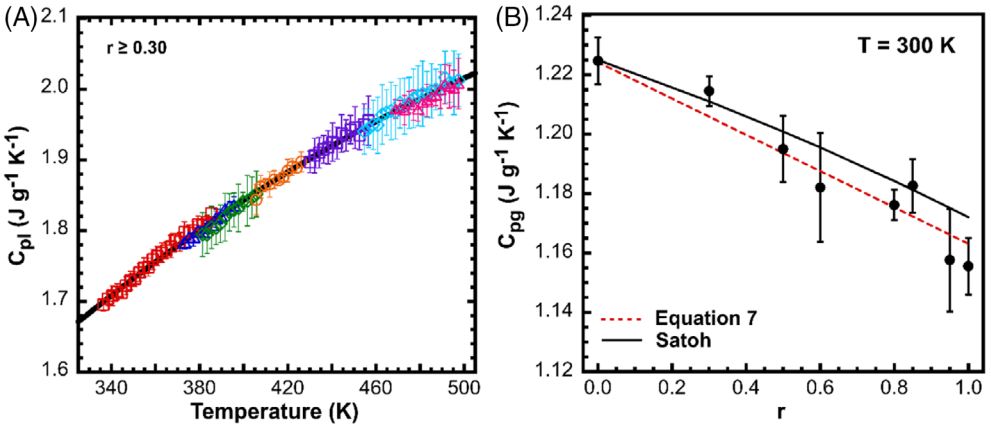

FIGURE 3 (A) Liquid heat capacity, C_{pl}, for cyanurates with $r \geq 0.3$ versus temperature, showing the second-order polynomial fit that describes all of the values, independent of composition. (B) Glassy heat capacity, C_{pg}, at 26.8°C for cyanurates as a function of composition, as well as the prediction from the group contribution method of Satoh.[55]

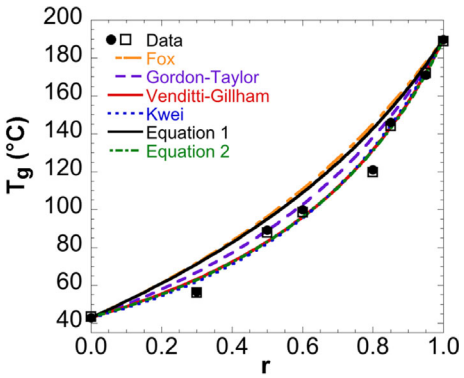

FIGURE 4 Experimental T_g data from dynamic DSC obtained at 10 K/min after cooling at 10 K/min (closed symbols) and step-scan (open symbols) as a function of the fraction r of cyanate ester groups belonging to the difunctional cyanate. Also shown are six fits to the data, including the numerical solution of Equation (1) using experimental values of liquid and glassy heat capacities for $r = 0.0$ and 1.0, the fits to the Fox, Gordon–Taylor, Venditti–Gillham, and Kwei equations, with the latter using the value of k determined from the experimental data, and the fit to Equation (2).

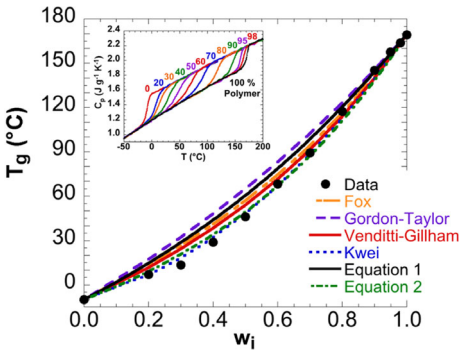

FIGURE 5 Experimental T_g data for poly(α-methyl styrene)/pentamer blends from step-scan DSC as a function of the weight fraction w_i of polymer. Also shown are five fits to the data, including the numerical solution of Equation (1) using the temperature-dependent value of ΔC_p reported in the text, as well as fits to the Fox, Gordon–Taylor, Venditti–Gillham, and Kwei equations, with the latter using the value of k determined from the experimental data. The inset shows the absolute C_p data for all blends, which shows that $\Delta C_p = C_{pl} - C_{pg}$ depends on temperature but not on composition in this ideal system.

using the temperature-dependent values of liquid and glassy heat capacities for dicyanate ester fractions $r = 0.0$ and 1.0, as given in Equations (5)–(7). Also shown in Figure 4 are fits to the equations in Table 1 using the experimentally determined value of k ($=\Delta C_{p2}/\Delta C_{p1} = 0.401/0.219 = 1.76$) for the Gordon–Taylor (GT), Venditti–Gillham (VG), and Kwei equations. The Venditti–Gillham equation describes the data very well with no adjustable parameters and is essentially equivalent to a best fit using a third-order polynomial. This is notwithstanding the fact that ΔC_p is not independent of temperature, as shown in Figure 2, which was one of the assumptions in the VG derivation. Furthermore, explicitly using the temperature dependent $\Delta C_p(T) = C_{pl}(T) - C_{pg}(T)$ in Equation (1) and numerically integrating results in a much worse description of the data. Interestingly, identically good fits to the VG equation are obtained using the Kwei equation (having one fitting parameter, $q = -28.8$ K) and using Equation (2), also with one fitting parameter: $S_c^E = 0.0482\, x_1 x_2$. Implications are further addressed in the discussion.

The T_g versus composition data for poly(α-methyl styrene)/pentamer blends is shown in Figure 5 as a function of the weight fraction w_i of polymer, with the inset showing the absolute heat capacity data for the blends. T_g monotonically increases from −10.1°C for the pure pentamer to 169.2°C for the pure polymer. The liquid and glassy heat capacities (inset) are independent of composition, indicating an ideal mixture from the thermodynamic point of view with no excess enthalpy or entropy. However, both liquid and glassy heat capacities do depend on temperature, such that $\Delta C_p = C_{pl} - C_{pg}$ follows a quadratic temperature dependence:

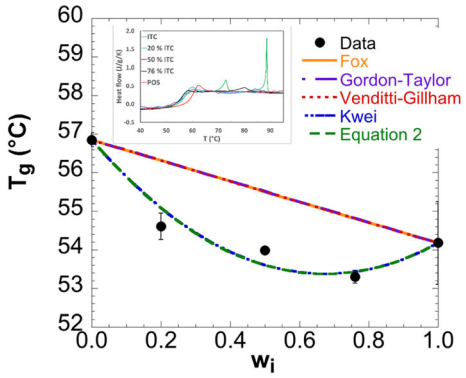

FIGURE 6 Experimental T_g data for the ITC/POS blends from dynamic DSC obtained at 10 K/min after cooling at 10 K/min as a function of the weight fraction w_i of ITC, with an inset showing the heat flow from DSC for the five samples investigated. Also shown are the Fox, Gordon–Taylor, and Venditti–Gillham equations, all of which have no adjustable parameters and are equivalent for this system, whereas the Kwei expression and that from Equation (2) each have one adjustable parameter, better describe the data, and are equivalent with one another.

$$\Delta C_p\left(\mathrm{J g^{-1}\,K^{-1}}\right) = 0.8841 - 2.733\mathrm{x}10^{-3}\,T + 3.072\mathrm{x}10^{-6}\,T^2 \tag{8}$$

where temperature has units of K. Similar to the case of the cyanurates, the Venditti–Gillham equation, with the parameter k determined from the experimental data at T_g and taken as constant ($k = \Delta C_{p2}/\Delta C_{p1} = 0.378/0.272 = 1.39$) describes the data best when considering equations where there is no adjustable parameter. Again, this is despite the fact that ΔC_p clearly is a function of temperature (as shown by the absolute heat capacity data in the inset) which is contrary to the assumption in the derivation of the Venditti–Gillham equation that ΔC_{p1} and ΔC_{p2} are constants, independent of temperature. On the other hand, direct integration of the heat capacity data using Equation (1) does not describe the T_g values nearly as well. The best fits of the poly(α-methyl styrene)/pentamer data are given by the Kwei equation and by Equation (2), both of which have an adjustable parameter, which ostensibly reflects nonideal interactions (e.g., excess entropy or enthalpy), with the Kwei parameter $q = -67.4$ K and the $S_c^E = 0.0432\,x_1x_2$ in Equation (2). This is in spite of the fact that nonidealities are not expected to be present in this system.

The T_g versus composition behavior of the itraconazole (ITC)/posaconazole (POS) blends is shown in Figure 6, with the inset showing the DSC heat flow data for the five compositions investigated on heating at 10 K/min after cooling at 10 K/min. It is clear from the inset that in addition to the small changes in T_g at around 55–60°C, the liquid crystalline behavior changes with composition. POS shows no liquid crystalline behavior, whereas ITC shows strong smectic and nematic liquid crystal melting peaks in the liquid state at temperatures of 70.8 ± 0.2 and 88.2 ± 0.1°C, respectively, consistent with values reported in the literature.[46–48] The liquid crystalline peaks decrease in intensity and shift to lower temperatures for the 76% ITC sample and then are not present in the other two blends. The T_g behavior for the ITC/POS system is not well described by the Fox, Gordon–Taylor, or Venditti–Gillham equations with the parameter k taken from the experimental data to be 1.0 for the latter two cases, and all three of these equations are equivalent given the narrow range of temperatures involved. Better fits are given by the Kwei equation with parameter $q = -4.2$ K and by Equation (2) (assuming here that ΔC_p = constant given the data shown in the inset and the small range of temperatures) with $S_c^E = 0.012\,x_1x_2$. The Kwei equation and Equation (2) give equivalently acceptable fits.

5 | DISCUSSION

In addition to changes in the glass transition temperature due to compositional changes, both the breadth and the cooling rate dependence of T_g can change. A question is whether or not these issues may be related to or the cause of the inability of Equation (1) to correctly predict the T_g as a function of composition for these three nearly ideal systems. It has long been recognized that the breadth of the glass transition increases dramatically in thermosetting systems near the point of gelation where the polydispersity and composition heterogeneity are broadest, and this is shown in Figure 2 (i.e., near compositions of $r = 0.6$ and 0.8). Similarly, the polymer/oligomer blend shows considerable broadening in temperature scans at intermediate compositions, as shown in the inset of Figure 5, although this broadening was not observed in dynamic rheological data.[47] On the other hand, the breadth of the glass transition region of the ITC/POS blends is not significantly affected by blending, as shown in the inset of Figure 6. One explanation for this difference may be the more dynamically heterogeneous environment in the polymeric systems due to chain connectivity[48,56] or concentration fluctuations,[57–59] but the lack of broadening in the ITC/POS system may also be due to the similarity of the two T_gs. In any case, suffice to say, that the changing breadth of the glass transition cannot be responsible for the inability of the additivity of configurational entropy to hold.

The temperature dependence of the segmental dynamics is also known to be influenced by composition. One measure of this temperature dependence is the cooling rate dependence of T_g, which is shown in Figure 7 for the three

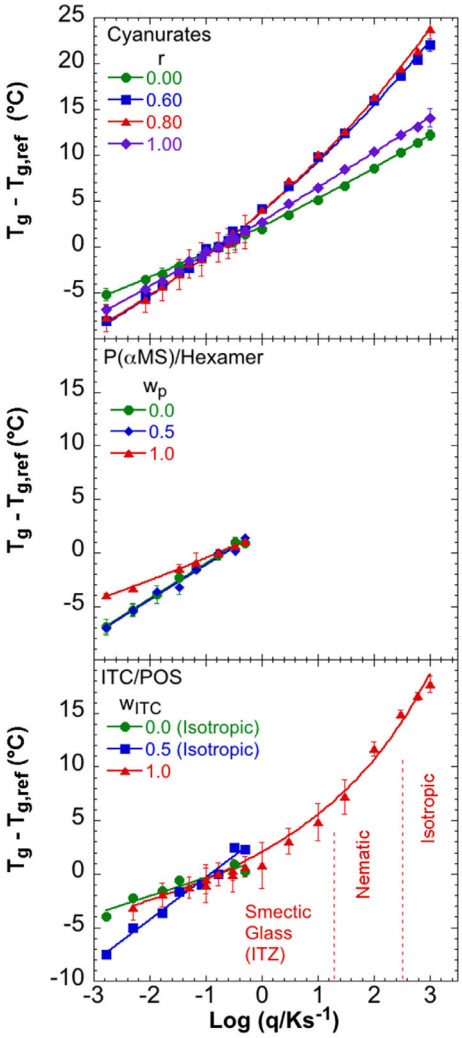

FIGURE 7 $T_g - T_{g,ref}$ versus logarithmic cooling rate for the three systems studied, showing the extreme compositions at r or $w_i = 0.0$ and 1.0 and one or two intermediate compositions for the sake of clarity. Experiments were performed using the Flash DSC for the cyanurates and the pure ITC, thereby extending the cooling rate range to 1000 K/s

systems investigated, where we plot $T_g - T_{g,ref}$ versus logarithm of cooling rate, where $T_{g,ref}$ is taken to be the value at a reference cooling rate $q_{ref} = 10$ K/min. Only one or two intermediate compositions are shown for each system for the sake of clarity. The systems show the typical Williams–Landel–Ferry (WLF)[60] temperature dependence of glass-forming materials when measured over a wide enough range of cooling rates:

$$\log\left(\frac{q}{q_{ref}}\right) = \frac{C_1(T_g - T_{g,ref})}{C_2 + T_g - T_{g,ref}} \quad (9)$$

where C_1 and C_2 are the WLF constants. It is apparent that cooling rate dependence is larger for the intermediate

TABLE 3 WLF fitting parameters and fragility values for the cyanurates

r	$T_{g,ref}$ (°C)	C_1	C_2 (K)	m
0.00	42.9 ± 1.1	104 ± 0.36	316 ± 1.1	105 ± 0.63
0.30	57.0 ± 7.9	16.0 ± 0.38	62.0 ± 1.7	85.3 ± 3.7
0.50	89.1 ± 8.0	18.7 ± 0.41	78.5 ± 2.0	86.3 ± 3.5
0.60	100 ± 7.8	18.1 ± 0.38	84.3 ± 2.0	80.0 ± 3.0
0.80	122 ± 7.8	14.5 ± 0.29	67.6 ± 1.6	84.7 ± 3.1
0.85	147 ± 7.0	13.6 ± 0.23	62.0 ± 1.2	92.3 ± 2.8
0.95	171 ± 9.4	22.2 ± 0.47	96.5 ± 2.3	102 ± 3.9
1.00	190 ± 0.63	128 ± 0.17	463 ± 0.63	128 ± 0.30

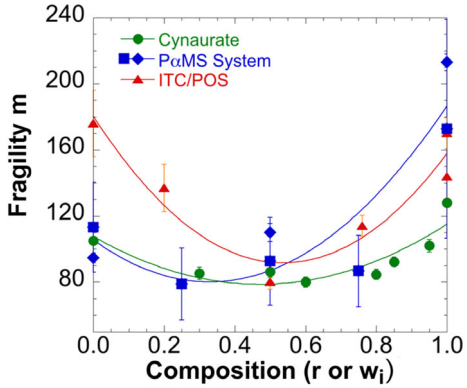

FIGURE 8 Fragility as a function of composition for the three systems examined. The PαMS/oligomer data include both fragility determined from the cooling rate dependence of T_g (squares) and rheological data (diamonds) from ref.[47]

compositions for the case of the cynaurates and the ITC/POS systems; for the polymer/oligomer system, the hexamer and 50/50 blend show a similar cooling rate dependence, larger than that of the polymer. The implication is that T_g of the blends will change more with a change in cooling rate than will the pure components, and hence, the degree of failure of Equation (1) will depend on the cooling rate chosen for the measurements. Furthermore, the fact that the cooling rate dependence of T_g depends on composition indicates that the difference between T_g measured at a finite rate and the value of the Gibbs and DiMarzio ideal glass transition temperature T_2 (assuming that it exists) will also depend on composition. The WLF C_2 values are often assumed to be a measure of the difference between T_g and T_2 since the equation predicts a divergence C_2 degrees below T_g. As shown in Table 3, the C_2 values for the cyanurates range from $T_{g,ref}$ (in K, and indicating Arrhenius behavior) for $r = 0.0$ and 1.0 down to values as low as 62–96 K for intermediate compositions.

Another measure of the temperature dependence of the dynamics is the fragility, $m = \mathrm{dlog}\ \tau/\mathrm{d}(T_g/T)$, which can be obtained from the WLF fit: $m = C_1 T_{g,\mathrm{ref}}/C_2$ or simply from the slope of T_g versus logarithm q: $m = (1/T_{g,\mathrm{ref}})/(\mathrm{d}T_g/\mathrm{dlog\ q})$.[23–27] The fragilities of the materials examined are plotted in Figure 8. First, we observe that the polycyanurate networks are of intermediate fragility even for the small molecule trimer ($r = 1.0$) with $m = 128$, whereas both the ITC and POS have high fragilities (140–180) in spite of their molecular nonpolymeric nature. We also see that for all of the systems, fragility decreases at intermediate compositions, although the degree of the change depends on the system. Simulations of polymers with flexible oligomers also indicate a decrease in fragility,[33] as do simulations of polymers and small molecule antiplasticizers.[31,32] Our result showing a minimum as a function of composition is intriguing in and of itself, and the reason for and generality of this behavior is not known. As mentioned in the Introduction, fragility has been related to the efficiency of molecular packing in polymers,[28] as well as to the relative stiffness of the side groups relative to the backbone.[29] We also note that although the T_g increases monotonically in these systems with composition, the temperature dependence of the relaxation time is nonmonotonic with composition. The latter decreases and goes through a minimum at intermediate compositions as the heterogeneity in the systems increase, and a similar result was observed for blends of polystyrenes of differing molecular weights.[61] Hence, for a given T_g value, systems with increased heterogeneity seem to show lower fragility values, a detail that is not captured in the general picture[25] of fragility increasing with T_g.

The main point, though, related to our tests of configurational entropy models is that the change in fragility indicates that the extrapolated temperature where the timescale of the dynamics will diverge to infinity will not be the same distance from the T_g measured at 10 K/min for all materials, which is one of the assumptions that Gordon and coworkers[6] made in deriving Equation (1). However, we argue that this is not the reason for the failure of Equation (1), because as shown by Couchman,[8–10] the equation can also be derived by assuming continuity of entropy in the liquid and glassy states at T_g. Furthermore, at slower cooling rates, deviations between the data and Equation (1) will be larger even though at slower cooling rates, T_g is closer to T_2 (assuming its existence).

As mentioned in the Introduction, McKenna and Simon used the PαMS/pentamer data to prove the lack of existence of an ideal glass transition temperature T_2.[45] Moreover, in a series of works on ultrastable glasses, ranging from 20 M-year-old amber to vacuum pyrolysis deposited Teflon, McKenna and coworkers[62–66] have shown that the relaxation times in the equilibrium state do not diverge even at temperatures as low as the Kauzmann temperature T_K (which has long been equated to the ideal glass transition temperature). These works provide strong evidence that the dynamics do not diverge at an ideal glass transition temperature and are consistent with computational and modeling works[16,67–70] that show that the configuration entropy does not go to zero at T_2, although there is a suggestion in recent work that it may plateau at low temperatures.[16] Hence, the underlying assumptions that the configurational entropy is invariant at the experimentally measured T_g and that the mixture T_g can be obtained from Equation (1) is called into question. If configurational entropy does plateau at T_2, its value would not necessarily be expected to be constant even for a homologous series of materials. The fact that Equation (1) does not work when directly tested using absolute heat capacity data for thermodynamically ideal mixtures gives strong support to this claim.

Finally, we point out an interesting observation in the T_g versus cooling rate relationship of the pure ITC: the relationship appears to be independent of the type of glass formed. ITC generally forms a liquid crystalline smectic glass, as shown in the conventional DSC scan in the inset of Figure 6. However, when it is cooled rapidly, as in the Flash DSC from 300 to 1000 K/s, ITC does not have time to form liquid crystalline domains and the resulting glass is an isotropic glass, as shown in SI and to be discussed in future work.[71] Moreover, at intermediate cooling rates, from 20 to 300 K/s, ITC forms a nematic glass. These three regimes are shown in the lower panel of Figure 7. On the other hand, both POS and the 50/50 blend form isotropic glasses. Several researchers have suggested that liquid crystalline glasses and isotropic glasses have different glass transition temperatures due to the structure of the glass; however, here, we argue that the differences are simply due to the differences in the rate at which the glass is cooled. For example, Tokita et al.[72] reported a T_g of 81°C for a main-chain polyester that formed a smectic glass at a cooling rate of 1 K/min, whereas the isotropic glass obtained on cooling at 100 K/min displayed a T_g of 93°C. The differences are similar to what we observe for ITC, in that the isotropic glasses have T_gs above 70°C, whereas the smectic glass formed at 10 K/s has a T_g some 10 K lower, which is expected for a change in cooling rate of over two decades. Furthermore, given that the cooling rate dependence of the glass transition is the same for the smectic ITC as for the isotropic POS, we suggest that the reason for the difference is solely due to difference in cooling rates and is not attributable to differences in glass structure on the molecular level.

6 | CONCLUSION

The composition dependence of the glass transition temperature (T_g) is examined using three model systems, oligomeric/polymeric cyanurates, blends of poly

(α-methyl styrene) and its oligomer, and molecular mixtures of itraconazole (ITC) and posaconazole (POS). We use absolute heat capacity data to test, for the first time, the assumption that the configurational entropies of the component materials are additive and that the configurational entropy is zero or unchanged at the T_g of the mixture relative to that at T_gs of the pure components. In addition, we examine several models of T_g as a function of composition that have a basis in configurational entropy ideas. We find that although the temperature-dependent heat capacities in both liquid and glassy states are nearly independent of composition for several of the systems studied, that is, the mixtures are nearly ideal systems in the thermodynamic sense, the mixture T_g is not well described by models based on the assumption that the configurational entropy, as given by the integral of $\Delta C_p d\ln T$, is zero or a constant at the glass transition temperature. In addition, we show that although T_g temperature-broadening occurs at intermediate compositions, this broadening cannot be the cause of the failure of the configurational entropy equation. We also show that the T_g dependence on cooling rate changes with composition and that the fragility m seems to decrease at intermediate compositions where the system is more heterogeneous. However, we argue that this is not the cause of the failure in the configurational entropy equation for mixture T_g although it does invalidate the assumption that T_g and T_2 have the same composition dependence. Finally, we point out that the differences in T_g in liquid crystalline and isotropic itraconazole glasses are attributable to differences in the cooling rate used to form the glasses rather than due to differences in the molecular structure of the glass itself.

ACKNOWLEDGMENTS

The authors gratefully acknowledge funding from NSF CMMI 1662046, DMR 1006972 and DMR 2105065.

DATA AVAILABILITY STATEMENT

Data is available on reasonable request from the corresponding author.

ORCID

Sindee L. Simon https://orcid.org/0000-0001-7498-2826

REFERENCES

[1] H. A. Schneider, *J. Res. Natl. Inst. Stand. Technol.* **1997**, *102*, 229.
[2] D. J. Plazek, K. L. Ngai, Ch. 12. in *Physical Properties of Polymers Handbook* (Ed: J. E. Mark), AIP Press, Woodbury, NY **1996**, p. 139.
[3] R. Pinal, *Entropy* **2008**, *10*, 207.
[4] J. M. Gordon, G. B. Rouose, J. H. Gibbs, W. M. Risen, *J. Chem. Phys.* **1977**, *66*(11), 4971.
[5] T. G. Fox, *Bull. Am. Phys. Soc.* **1965**, *1*, 123.
[6] M. Gordon, J. S. Taylor, *J. Appl. Chem.* **1952**, *493-500*, 493.
[7] F. N. Kelley, F. Bueche, *J. Polym. Sci.* **1961**, *50*(154), 549.
[8] P. R. Couchman, F. E. Karasz, *Macromolecules* **1978**, *11*(1), 117.
[9] P. R. Couchman, *Macromolecules* **1978**, *11*(6), 1156.
[10] P. R. Couchman, *Polym. Eng. Sci.* **1984**, *24*(2), 135.
[11] R. A. Venditti, J. K. Gillham, *J. Appl. Polym. Sci.* **1997**, *64*, 3.
[12] V. E. Jenckel, R. Heusch, *Kolloid- Zeitschrift* **1953**, *130*(2), 89.
[13] G. Braun, A. J. Kovacs, *Phys. Non-Crystall. Solids* **1965**, *303*, 303.
[14] T. K. Kwei, *J. Polym. Sci., Polym. Lett. Ed.* **1984**, *22*, 307.
[15] J. H. Gibbs, E. A. Dimarzio, *J. Chem. Phys.* **1958**, *28*, 373.
[16] W. S. Xu, J. F. Douglas, Z. Y. Sun, *Macromolecules* **2021**, *54*(7), 3001.
[17] C. A. Angell, R. D. Bressel, *J. Phys. Chem.* **1972**, *76*(22), 3244.
[18] J. M. Smith, H. Van Ness, M. Abbott, *Introduction to Chemical Engineering Thermodynamics*, 7th ed., McGraw-Hill, Massachusetts: McGraw-Hill, **2004**.
[19] X. Zhao, S. X. Cheng, Y. P. Koh, B. D. Kelly, G. B. McKenna, S. L. Simon, *Mol. Pharm.* **2021**, *18*(9), 3439.
[20] R. J. Babu, W. Brostow, O. Fasina, I. M. Kalogeras, S. Sathigari, A. Vassilikou-Dova, *Polym. Eng. Sci.* **2011**, *51*(8), 1456.
[21] I. M. Kalogeras, *Eur. J. Pharm. Sci.* **2011**, *42*(5), 470.
[22] M. Aubin, R. E. Prudhomme, *Polym. Eng. Sci.* **1988**, *28*(21), 1355.
[23] C. G. Robertson, P. G. Santangelo, C. M. Roland, *J. Non-Cryst. Sol.* **2000**, *275*, 153.
[24] I. Echeverria, P. L. Kolek, D. J. Plazek, S. L. Simon, *J. Non-Crys. Sol.* **2003**, *324*, 242.
[25] J. Zhao, G. B. McKenna, *Polymer* **2014**, *55*, 2246.
[26] S. L. Simon, Y. P. Koh, in *Fast Scanning Calorimetry* (Eds: C. Schick, V. Mathot), Springer, Switzerland **2017**, p. 433.
[27] C. A. Angell, *J. Non-Cryst. Solids* **1991**, *131-133*, 13.
[28] J. Dudowicz, K. F. Freed, J. F. Douglas, *J. Phys. Chem. B* **2005**, *109*, 21350.
[29] K. Kunal, C. G. Robertson, S. Pawlus, S. F. Hahn, A. P. Sokolov, *Macromolecules* **2008**, *41*, 7232.
[30] C. Dalle-Ferrier, A. Kisliuk, L. Hong, G. Carini, G. Carini, G. D'Angelo, C. Alba-Simionesco, V. N. Novikov, A. P. Sokolov, *J. Chem. Phys.* **2016**, *145*, 154901.
[31] R. A. Riggleman, J. F. Douglas, J. J. de Pablo, *Phys. Rev. E* **2007**, *7*(1), 011504.
[32] R. A. Riggleman, J. F. Douglas, J. J. de Pablo, *Soft Matter* **2010**, *6*(2), 292.
[33] J. H. Mangalara, D. S. Simmons, *ACS Macro Lett.* **2015**, *4*, 1134.
[34] Q. Qin, G. B. McKenna, *J. Non-Cryst. Solids* **2006**, *352*, 2977.
[35] T. Wang, O. Gulbiten, R. Wang, Z. Yang, A. Smith, B. Luther-Davies, P. Lucas, *J. Phys. Chem. B* **2014**, *118*, 1436.
[36] C. Yildirim, J.-Y. Raty, M. Micoulaut, *Nat. Commun.* **2016**, *7*, 11086.
[37] S. L. Simon, J. K. Gillham, *J. Appl. Polym. Sci.* **1993**, *47*, 461.
[38] Y. P. Koh, S. L. Simon, *J. Phys. Chem. B* **2010**, *114*, 7727.
[39] D. R. Miller, C. W. Macosko, *Macromolecules* **1976**, *9*, 206.
[40] A. M. Gupta, C. W. Macosko, *Macromolecules* **1993**, *26*, 2455.
[41] R. H. Lin, J. L. Hong, A. C. Su, *Comp. Theor. Polym. Sci.* **1997**, *1997*(7), 95.
[42] R. H. Lin, A. C. Su, J. L. Hong, *J. Appl. Polym. Sci.* **1999**, *73*, 1927.
[43] Q. X. Li, S. L. Simon, *Macromolecules* **2007**, *40*, 2246.

[44] D. Huang, S. L. Simon, G. B. McKenna, *J. Chem. Phys.* **2005**, *122*, 84907.
[45] S. L. Simon, G. B. McKenna, *J. Non-Cryst. Solids* **2009**, *355*, 672.
[46] W. Zheng, S. L. Simon, *J. Polym. Sci., Part B: Polym. Phys.* **2008**, *46*, 418.
[47] W. Zheng, G. B. McKenna, S. L. Simon, *Polymer* **2010**, *51*, 4899.
[48] T. P. Lodge, T. C. B. McLeish, *Macromolecules* **2000**, *33*, 5278.
[49] K. Six, G. Verreck, J. Peeters, K. Binnemans, H. Berghmans, P. Augustijns, R. Kinget, G. Van den Mooter, *Thermochim. Acta* **2001**, *376*(2), 175.
[50] M. Tarnacka, K. Adrjanowicz, E. Kaminska, K. Kaminski, K. Grzybowska, K. Kolodziejczyk, P. Wlodarczyk, L. Hawelek, G. Garbacz, A. Kocot, M. Paluch, *Phys. Chem. Chem. Phys.* **2013**, *15*(47), 20742.
[51] E. U. Mapesa, M. Tarnacka, E. Kaminska, K. Adrjanowicz, M. Dulski, W. Kossack, M. Tress, W. K. Kipnusu, K. Kaminski, F. Kremer, *RSC Adv.* **2014**, *4*(54), 28432.
[52] C. T. Moynihan, P. B. Macedo, C. J. Montrose, P. K. Gupta, M. A. DeBolt, J. F. Dill, B. E. Dom, P. W. Drake, A. J. Easteal, P. B. Elterman, *Ann. N. Y. Acad. Sci.* **1976**, *279*(1), 15.
[53] P. Badrinarayanan, W. Zheng, Q. X. Li, S. L. Simon, *J. Non-Cryst. Sol.* **2007**, *353*, 2603.
[54] J. E. K. Schawe, *Thermochim. Acta* **2015**, *603*, 128.
[55] S. Satoh, *J. Sci. Res. Inst.* **1948**, *43*, 79.
[56] G. C. Chung, J. A. Kornfield, S. D. Smith, *Macromolecules* **1994**, *27*, 96.
[57] A. Zetsche, E. W. Fischer, *Acta Polm* **1994**, *45*, 168.
[58] S. Salaniwal, R. Kant, R. H. Colby, S. K. Kumar, *Macromolecules* **2002**, *35*, 9211.
[59] S. Y. Kamath, R. H. Colby, S. K. Kumar, *Phys. Rev. E* **2003**, *67*, 010801.
[60] M. L. Williams, R. F. Landel, J. D. Ferry, *J. Am. Chem. Soc.* **1955**, *77*, 3701.
[61] C. Dalle-Ferrier, S. Simon, W. Zheng, P. Badrinarayanan, T. Fennell, B. Frick, J. M. Zanotti, C. Alba-Simionesco, *Phys. Rev. Lett.* **2009**, *103*, 185702.
[62] J. Zhao, S. L. Simon, G. B. McKenna, *Nat. Commun* **2013**, *4*, 1783.
[63] H. D. Yoon, Y. P. Koh, S. L. Simon, G. B. McKenna, *Macromolecules* **2017**, *50*(11), 4562.
[64] G. B. McKenna, J. Zhao, *J. Non-Cryst. Solids* **2015**, *407*, 3.
[65] H. Yoon, G. B. McKenna, *Sci. Adv.* **2018**, *4*(12), eaau5423.
[66] D. J. Chen, G. B. McKenna, *J. Non-Cryst. Solids* **2021**, *566*, 120871.
[67] A. Milchev, *Dokl. Bulg. Akad. Nauk.* **1983**, *36*, 1415.
[68] A. Donev, F. H. Stillinger, S. Torquato, *J. Chem. Phys.* **2007**, *127*, 124509.
[69] J. Baschnagel, M. Wolfgardt, W. Paul, K. Binder, *J. Res. Natl. Inst. Stand. Technol.* **1997**, *102*, 159.
[70] M. Wolfgardt, J. Baschnagel, W. Paul, K. Binder, *Phys. Rev. E.* **1996**, *54*, 1535.
[71] J. A. Zapata-Hincapie, L. Grassia, S. L. Simon, in preparation.
[72] M. Tokita, S. Funaoka, J. Watanabe, *Macromolecules* **2004**, *37*(26), 9916.

SUPPORTING INFORMATION

Additional supporting information may be found in the online version of the article at the publisher's website.

How to cite this article: E. Lopez, Y. P. Koh, J. A. Zapata-Hincapie, S. L. Simon, *Polym. Eng. Sci.* **2022**, 1. https://doi.org/10.1002/pen.26018